

Structure and transport properties of the $\text{Fe}_{0.5}\text{Ni}_{0.5}$ composite

G. Ya. Khadzhai¹, S. R. Vovk^{2,3}, R. V. Vovk¹, E. S. Gevorkyan^{1,2}, M. V. Kislitsa¹,
A. Feher³, P. Kollar³, and J. Fuzer³

¹*V. N. Karazin Kharkiv National University, Kharkiv 61022, Ukraine*

E-mail: gkhadjai@gmail.com;

rvvovk2017@gmail.com

²*Ukrainian State University of Railway Transport, Kharkiv 61050, Ukraine*

³*Faculty of Science, P. J. Safarik University, Kosice 041 54, Slovakia*

Received October 28, 2020, revised November 29, 2020, published online December 25, 2020

It is shown that the experimental data on the temperature dependences of the effective electrical resistance and thermal conductivity in the range of 4.2–300 K of the electroconsolidated $\text{Fe}_{0.5}\text{Ni}_{0.5}$ composite are within the Hashin–Shtrikman boundaries for the conductivities of a three-phase system. The components of the system are pure Fe and Ni, and the intergranular medium in the form of an alloy with an average composition close to $\text{Fe}_{0.5}\text{Ni}_{0.5}$ is considered as the third phase.

Keywords: electroconsolidated composite, electrical resistance, thermal conductivity, Hashin–Shtrikman boundaries, three-phase system, intergranular medium.

The creation of promising functional materials with desired properties often requires the use of new technologies for their production [1–5], including a combination of modern methods for modeling their structural and magnetoresistive characteristics [6, 7] and the use of the latest intensive synthesis techniques [8–10]. In particular, the development of powder metallurgy is associated with intensive compaction methods, where, along with pressure and temperature, field and direct action of electric current are actively used. Such electroconsolidation [11] provides a high-density and finely dispersed structure of the composite [12], and also provides cleaning and activation of the surface of sintered powders, which significantly contributes to both the chemical purity of the final product and the compaction of sintered powders [13].

A very promising class of modern functional materials is composite soft magnetic materials, in particular, materials based on iron-nickel compounds [8, 14, 15]. These compounds possess a unique combination of properties of metals and ceramics, such as high hardness, refractoriness and elasticity, as well as good thermal and electrical conductivity [15, 16]. When synthesizing such materials by the method of electroconsolidation, as a rule, the volume fractions of the components and their properties are known. The corresponding functional properties of the resulting composite, including magnetic, are determined by the pro-

perties of all components, their volume fractions, the shape and spatial distribution of the constituent phases, inter-phase boundaries and other characteristics. The materials obtained in this way are spatially inhomogeneous, and predicting their properties in a wide range of external influences is a nontrivial problem.

The study of the mechanisms of electrical and heat transfer in these compounds provides an important tool for checking the adequacy of numerous theoretical models and searching for empirical ways to improve their technological characteristics.

This work is devoted to establishing a relationship between the structure of the Fe–Ni metal composite obtained by the electroconsolidation method and experimental data on its effective electrical and thermal conductivity in the range of 4.2–300 K.

The samples were obtained by electroconsolidation from nickel (PNE-45–200 μm , nickel content 99.9%) and iron (sprayed PZhR 2.200.28, iron content 99.9%) with a grain size of about 200 μm . Electroconsolidation was carried out for 10 min at 1100 °C, pressure 35 MPa and current ~ 5 kA. The heating rate was ~ 200 °C/min. The investigated composite sample had the shape of a rectangular bar with dimensions 15×4×6 mm.

The surface of the sample was carefully polished and examined in a Tescan Vega 3LMH scanning electron mi-

croscope equipped with a Bruker XFlash 5010 EDS characteristic x-ray detector.

Sample resistance, $\rho(T)$, was measured by the standard 4-contact method. Thermal conductivity, $\lambda(T)$, was determined by the method of stationary uniaxial heat flux. The temperature range of measurements is 4.2–300 K.

When synthesizing a multiphase material, a very important question is whether one or another effective characteristic of a multiphase material is completely determined by the volume fractions and the corresponding characteristics of the constituent phases.

In [14] a negative answer was given to this question, and instead of an expression for the effective characteristic, expressions were obtained for the upper and lower boundaries of the studied characteristic — the Hashin–Shtrikman boundary. The relations obtained in [14] are valid for the magnetic permeability, and also, by analogy, for the dielectric constant, thermal and electrical conductivity, and diffusion coefficient.

Thus, if only the volume fractions and the corresponding characteristics of the constituent phases are known for a multiphase material, then it is possible to determine only the boundaries within which the corresponding effective characteristics of the material are located [14].

Note that the widest limits of the conductivity of a multiphase system — the worst case — are given by parallel and series alignment of phases.

In general, the narrowest boundaries obtained in [14] have the form

$$\sigma_l^* \geq \sigma_l + \frac{A_l}{1 - A_l / (3\sigma_l)}, \quad A_l = \sum_{t=2}^n \frac{v_t}{(\sigma_t - \sigma_l)^{-1} + (3\sigma_l)^{-1}}, \quad (1)$$

$$\sigma_l^* \leq \sigma_m + \frac{A_m}{1 - A_m / (3\sigma_m)}, \quad A_m = \sum_{t=2}^n \frac{v_t}{(\sigma_t - \sigma_m)^{-1} + (3\sigma_m)^{-1}}. \quad (2)$$

Here the index t ($t = 1, 2, 3, \dots, n$) numbers the phases in the order (for example) of increasing conductivity, i.e.,

from σ_l to σ_m ; v_t is the volume fraction of phase t , $\sum_{t=1}^n v_t = 1$.

For two-phase materials without significant scattering at the interphase boundaries, the obtained narrow conductivity boundaries are expressed directly in terms of the conductivity and volume fractions of the constituent phases [14, 15]:

$$\begin{aligned} \sigma_l^* &= \sigma_l + \frac{v_2}{(\sigma_2 - \sigma_l)^{-1} + v_1 / (3\sigma_l)}, \\ \sigma_m^* &= \sigma_m + \frac{v_1}{(\sigma_1 - \sigma_2)^{-1} + v_2 / (3\sigma_2)}, \quad \sigma_1 < \sigma_2. \end{aligned} \quad (3)$$

In [16], we investigated the electrical and thermal conductivity of the electroconsolidated Fe_{0.5}Ni_{0.5} composite in the range of 4.2–300 K. It turned out that both the electrical and thermal conductivity of the sample lie below the

curves for pure Fe and Ni [17, 18], but higher than for the Fe_{0.5}Ni_{0.5} alloy [17–19]. This means that the interparticle boundaries in the composite make a significant contribution to the scattering of heat and charge carriers, i.e., the electrical and thermal conductivity of the sample cannot be described by formula (3).

In [20], the surface of this sample was studied by a scanning electron microscope equipped with an EDS detector of characteristic x-ray radiation. This made it possible to determine the spatial distribution of Fe and Ni elements on the sample surface, and, based on these data, to estimate the coefficient of interdiffusion of iron and nickel in this system at the temperature of electroconsolidation (≈ 1100 °C).

It turned out that the width of the diffusion zone is about 60 μm , which is comparable with the initial grain size of Fe and Ni — ≈ 200 μm [20]. Then, in the roughest approximation, the volume fraction of pure Fe and Ni is $\approx 30\%$, i.e., the interparticle medium not only makes a significant contribution to the electrical and thermal resistance but also occupies 2/3 of the sample volume.

Thus, after electroconsolidation, the Fe_{0.5}Ni_{0.5} composite becomes a three-phase system and its conductivity should be described by formulas (1) for $n = 3$.

Denoting by σ_b the conductivity of the interparticle medium, arranging the conductivity in ascending order — $\sigma_1 < \sigma_2 < \sigma_3$, i. e., $\sigma_b < \sigma_{\text{Fe}} < \sigma_{\text{Ni}}$, and using (1), we have

$$\sigma_l^* = \sigma_b + \frac{A_b}{1 - A_b / (3\sigma_b)}, \quad (4)$$

$$A_b = \frac{v_{\text{Fe}}}{(\sigma_{\text{Fe}} - \sigma_b)^{-1} + (3\sigma_b)^{-1}} + \frac{v_{\text{Ni}}}{(\sigma_{\text{Ni}} - \sigma_b)^{-1} + (3\sigma_b)^{-1}},$$

$$\sigma_m^* = \sigma_{\text{Ni}} + \frac{A_{\text{Ni}}}{1 - A_{\text{Ni}} / (3\sigma_{\text{Ni}})}, \quad (5)$$

$$A_{\text{Ni}} = \frac{v_b}{(\sigma_b - \sigma_{\text{Ni}})^{-1} + (3\sigma_{\text{Ni}})^{-1}} + \frac{v_{\text{Fe}}}{(\sigma_{\text{Fe}} - \sigma_{\text{Ni}})^{-1} + (3\sigma_{\text{Ni}})^{-1}}.$$

It is assumed that $v_{\text{Ni}} = v_{\text{Fe}} \approx 0.17$, $v_b \approx 0.66$ according to the size of the diffusion zone.

We do not know the conductivity of the interparticle medium, σ_b , and it should be chosen so that the experimental data — the effective conductivities of the system — are inside the boundaries calculated by formulas (4), (5). Since the interparticle medium is formed due to interdiffusion between the particles of pure Fe and Ni, it is natural to assume that the composition of this medium corresponds to the composition of the Fe_{0.5}Ni_{0.5} alloy.

Figure 1 shows the boundaries calculated by formulas (4), (5) in the range of 4.2–300 K at $\sigma_{\text{Ni}}(T)$, $\sigma_{\text{Fe}}(T)$, and $\sigma_b(T)$ taken from [17, 18]. The dependence $\rho_b(T) = 1/\sigma_b(T)$ corresponds to the Fe_{0.51}Ni_{0.49} composition [17], and the dependence $\lambda(T)$ corresponds to the Fe_{0.46}Ni_{0.51} composition [18].

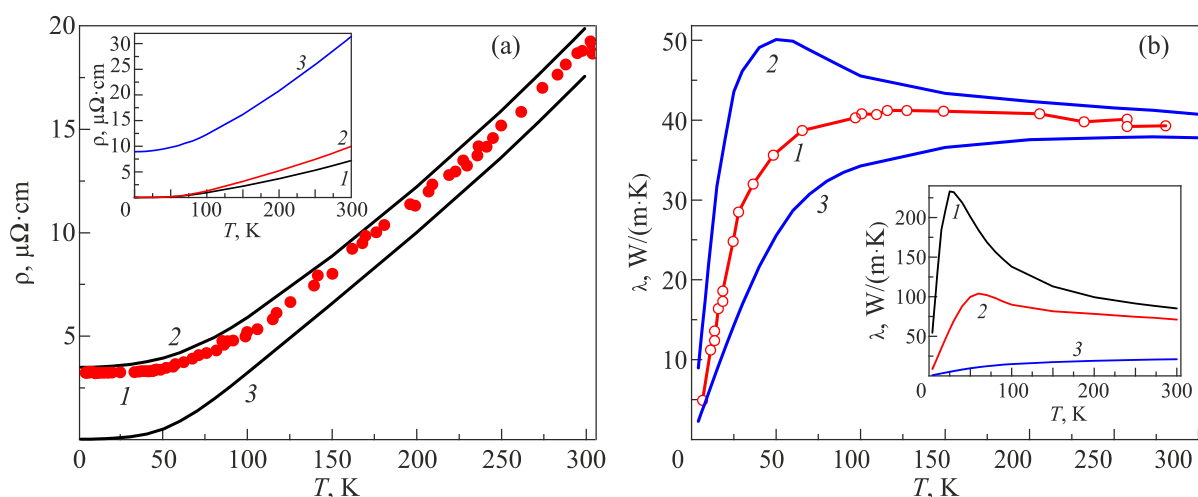


Fig. 1. Hashin–Shtrikman boundaries of electrical resistance (a) and thermal conductivity (b) of electroconsolidated equiatomic Fe–Ni composite: experiment (1), upper limit (2), lower limit (3). The insets show the initial data from [17, 18] for calculations according to the formula (1). Inset (a): $\rho(\text{Ni})$ (curve 1), $\rho(\text{Fe})$ (2), $\rho(\text{Fe}_{0.51}\text{Ni}_{0.49})$ (3). Inset (b): $\lambda(\text{Ni})$ (1), $\lambda(\text{Fe})$ (2), $\lambda(\text{Fe}_{0.46}\text{Ni}_{0.51})$ (3).

The corresponding experimental data are shown by dots. It can be seen that in the entire investigated temperature range the experimental data are within the boundaries calculated by formulas (4), (5). The insets show the temperature dependences $\rho_{\text{Ni}}(T) = 1/\sigma_{\text{Ni}}(T)$, $\rho_{\text{Fe}}(T) = 1/\sigma_{\text{Fe}}(T)$, $\rho_b(T) = 1/\sigma_b(T)$ [17] and $\lambda_{\text{Ni}}(T)$, $\lambda_{\text{Fe}}(T)$ and $\lambda_b(T)$ [18], in accordance with which the calculation was carried out by formulas (4), (5).

Thus, the Hashin–Shtrikman boundaries [formulas (3)–(5)] can be used to estimate the unknown conductivity of one of the phases if the volume fractions of all phases are known. These estimates are of particular interest if they are carried out for several characteristics (electrical and thermal conductivity) [15] and in a wide range of changes in some external parameter (temperature, pressure, etc.).

In this work, Hashin–Shtrikman boundaries were constructed for the conductivities of a three-phase system. The experimental results on the temperature dependences in the range of 4.2–300 K of the electrical resistance and thermal conductivity of the electroconsolidated $\text{Fe}_{0.5}\text{Ni}_{0.5}$ composite are within these boundaries, if the third phase is considered to be the intergranular medium, which is an alloy with an average composition of $\text{Fe}_{0.5}\text{Ni}_{0.5}$. Comparison of the Hashin–Shtrikman boundaries with experimental results at different temperatures allows one to estimate the unknown conductivity of one of the phases.

1. M. A. Hadi, R. V. Vovk, and A. Chroneos, *J. Mater. Sci.: Mater. Electronics* **27**, 11925 (2016).
2. A. L. Solovjov, E. V. Petrenko, L. V. Omelchenko, R. V. Vovk, I. L. Goulatis, and A. Chroneos, *Sci. Rep.* **9**, 9274 (2019).
3. A. L. Solovjov, L. V. Omelchenko, E. V. Petrenko, R. V. Vovk, V. V. Khotkevych, and A. Chroneos, *Sci. Rep.* **9**, 20424 (2019).

4. O. V. Dobrovolskiy, M. Huth, V. A. Shklovskij, and R. V. Vovk, *Sci. Rep.* **7**, 13740 (2017).
5. O. V. Dobrovolskiy, R. Sachser, T. Brächer, T. Fischer, V. V. Kruglyak, R. V. Vovk, V. A. Shklovskij, M. Huth, B. Hillebrands, and A. V. Chumak, *Nat. Phys.* **15**, 477 (2019), *arXiv:1901.06156*.
6. N. Kuganathan, P. Iyngaran, R. Vovk, and A. Chroneos, *Sci. Rep.* **9**, 4394 (2019).
7. N. Kuganathan, A. Kordatos, M. E. Fitzpatrick, R. V. Vovk, and A. Chroneos, *Solid State Ionics* **327**, 93 (2018).
8. E. A. Perigo, B. Weidenfeller, P. Kollar, and J. Fuzer, *Appl. Phys. Rev.* **5**, 031301 (2018).
9. R. V. Vovk and A. L. Solovjov, *Fiz. Nizk. Temp.* **44**, 111 (2018) [*Low Temp. Phys.* **44**, 81 (2018)].
10. O. V. Dobrovolskiy, V. M. Bevez, M. Yu. Mikhailov, O. I. Yuzepovich, V. A. Shklovskij, R. V. Vovk, M. I. Tsindlekht, R. Sachser, and M. Huth, *Nat. Commun.* **9**, 4927 (2018).
11. F. Bernard, S. Le Gallet, N. Spinassou, S. Paris, E. Gaffet, J. N. Woolman, and Z. A. Munir, *Sci. Sintering* **36**, 155 (2004).
12. D. L. Bourelland and J. R. Groza, *ASM Handbook*, Vol. 7, Powder Metallurgy (1998), p. 508.
13. E. Aslan, N. Camuşcu, and B. Birgören, *Materials & Design* **28**, Is. 5, 1618 (2007).
14. Z. Hashin and S. Shtrikman, *J. Appl. Phys.* **33**, 3125 (1962).
15. P. L. Rossiter, *The Electrical Resistivity of Metals and Alloys*, Cambridge University Press (1987).
16. G. Ya. Khadzhay, S. R. Vovk, R. V. Vovk, E. S. Gevorkyan, N. S. Zubenko, M. V. Kislitsa, B. O. Chishkala, A. Feher, P. Kollar, and J. Fuzer, *Fiz. Nizk. Temp.* **46**, 1110 (2020) [*Low Temp. Phys.* **46**, 939 (2020)].
17. C. Y. Ho, M. W. Ackerman, K. Y. Wu, T. N. Havill, R. H. Bogaard, R. A. Matula, S. G. Oh, and H. M. James, *J. Phys. Chem. Ref. Data* **12**, 183 (1983).

18. C. Y. Ho, M. W. Ackerman, K. Y. Wu, S. G. Oh, and T. N. Havill, *J. Phys. Chem. Ref. Data* **7**, 959 (1978).
19. K. Jin, B. Sales, G. Stocks, G. D. Samolyuk, M. Daene, W. J. Weber, Y. Zhang, and H. Bei, *Sci. Rep.* **6**, 20159 (2016).
20. V. Bogdanov, R. Vovk, E. Gevorkyan, S. Dukarov, M. Kislitsa, S. Petrushenko, V. Sukhov, and G. Khadzhai, *Electron Microscopic Study of Interdiffusion in an Equiatomic Fe–Ni Composite*, Accepted to Acta Physica Polonica A.

Структура та транспортні властивості
композиту $\text{Fe}_{0.5}\text{Ni}_{0.5}$

G. Ya. Khadzhai, S. R. Vovk, R. V. Vovk,
E. S. Gevorkyan, M. V. Kislitsa, A. Feher, P. Kollar,
J. Fuzer

Показано, що експериментальні дані по температурним залежностям ефективного електроопору та теплопровідності в діапазоні 4,2–300 К електроконсолідованого композиту $\text{Fe}_{0.5}\text{Ni}_{0.5}$ знаходяться в межах границь Хашіна–Штрікмана для провідностей трифазної системи. Компонентами системи є чисті Fe та Ni, а в якості третьої фази розглядається міжзернисте середовище у вигляді сплаву з середнім складом, близьким до $\text{Fe}_{0.5}\text{Ni}_{0.5}$.

Ключові слова: електроконсолідований композит, електричний опір, теплопровідність, границі Хашіна–Штрікмана, трифазна система, міжзернисте середовище.